energy**&fuels**
article

Chemical Structures of Swine-Manure Chars Produced under Different Carbonization Conditions Investigated by Advanced Solid-State ^{13}C Nuclear Magnetic Resonance (NMR) Spectroscopy[†]

Xiaoyan Cao,[‡] Kyoung S. Ro,[§] Mark Chappell,[‖] Yuan Li,[‡] and Jingdong Mao*,[‡]

[‡]*Department of Chemistry and Biochemistry, Old Dominion University, 4541 Hampton Boulevard, Norfolk, Virginia 23529, United States,* [§]*Coastal Plains Soil, Water, and Plant Research Center, Agricultural Research Service (ARS), United States Department of Agriculture (USDA), 2611 West Lucas Street, Florence, South Carolina 29501, United States, and* [‖]*Environmental Laboratory, United States Army Corps of Engineers (USACE), 3909 Halls Ferry Road, Vicksburg, Mississippi 39180, United States*

Received October 3, 2010. Revised Manuscript Received November 23, 2010

Two types of swine-manure chars, hydrothermally produced hydrochar and slow-pyrolysis pyrochar, and their raw swine-manure solid were characterized using advanced solid-state ^{13}C nuclear magnetic resonance (NMR) spectroscopy. In comparison to raw swine-manure solid, both hydrochars and pyrochar displayed significantly different structural features, with lower alkyl carbons, NCH, OCH$_3$, O-alkyl, and COO/N—C═O groups but higher aromatic/olefinic and aromatic C—O groups. The chemical structures of four hydrochars varied with different processing conditions. In comparison to the hydrochar with only water wash (HTC-swine W), washing hydrochar with acetone (HTC-swine A) removed the soluble intermediates deposited on the hydrochar, as shown by the decrease of O-alkyl (primarily carbohydrates), corresponding increase of aromatic/olefinic carbons and complete removal of OCH$_3$ groups. With citric acid prewash and acetone wash (HTC-AW-swine A), aromatic C—O and aromatics/olefinics were increased and alkyls were decreased, with O-alkyls totally removed in comparison to just acetone wash (HTC-swine A). Citric acid catalysis and acetone wash (HTC-AC-swine A) increased aromatic C—O and non-protonated aromatics/ olefinics, decreased alkyls further, and reduced protonated aromatics/olefinics compared to citric acid prewash and acetone wash (HTC-AW-swine A). The ratios of non-protonated to protonated aromatic/ olefinic carbons for HTC-swine W, HTC-swine A, and HTC-AW-swine A hydrochars were quite similar but enhanced for HTC-AC-swine A hydrochar. Obviously, citric acid catalysis and acetone wash (HTC-AC-swine A) provided deeper carbonization than other hydrothermal processes. Hydrothermal carbonization (HTC) processes were associated with the hydrolysis and subsequent decomposition of major biopolymer components in swine manure. The increase of aromaticity during HTC was likely due to condensation polymerization of the intermediates from the degradation of carbohydrates. Pyrochar produced from slow pyrolysis was structurally different from HTC hydrochars. The dominant component of pyrochar was aromatics, whereas that of hydrochars was alkyl moieties. The aromatic cluster size of pyrochar was larger than those of hydrochars. Slow pyrolysis at 620 °C provided deeper carbonization than HTC processes.

Introduction

The conversion of biomass, including agricultural crops, trees, animal manures, municipal residues, and other residues, into renewable energy products, such as combustible gases, liquids, and chars, has been extensively studied because of concerns over global warming and limited petroleum supplies.[1−3] A wide variety of biomasses (straw, marine microalgae, leaf, wood, bark, municipal solid waste, etc.) have been applied to produce bio-oil, biochar, and syngas, with the advantages of being CO$_2$-neutral, having low sulfur content, and being easy to store and transport.[4−11] Use of organic-based waste products, for example, animal manures, as feedstocks for biomass−bioenergy conversion processes is of particular importance with regard to its dual functions of waste reduction and energy production.[12] U.S. agricultural lands currently produce 35 million dry tons of sustainable animal manures,

(1) Perlack, R. D.; Wright, L. L.; Turhallow, A. F.; Graham, R. L.; Stokes, B. J.; Erbach, D. C. Biomass as a feedstock for a bioenergy and bioproducts industry: The technical feasibility of a billion-ton annual supply. *DOE/GO-102995-2135*; United States Department of Energy (DOE): Washington, D.C., April 2005.
(2) Bridgwater, T. *J. Sci. Food Agric.* **2006**, *86*, 1755–1768.
(3) Hayes, M. H. B. *Nature* **2006**, *443*, 144–144.
(4) Onwudili, J. A.; Williams, P. T. *Energy Fuels* **2007**, *21*, 3676–3683.
(5) Mullen, C. A.; Boateng, A. A.; Hicks, K. B.; Goldberg, N. M.; Moreau, R. A. *Energy Fuels* **2010**, *24*, 699–706.
(6) Brown, T. M.; Duan, P. G.; Savage, P. E. *Energy Fuels* **2010**, *24*, 3639–3646.
(7) Karaosmanoglu, F.; Isigigur-Ergundenler, A.; Sever, A. *Energy Fuels* **2000**, *14*, 336–339.
(8) Abdullah, H.; Wu, H. W. *Energy Fuels* **2009**, *23*, 4174–4181.
(9) Link, S.; Arvelakis, S.; Spliethoff, H.; De Waard, P.; Samoson, A. *Energy Fuels* **2008**, *22*, 3523–3530.
(10) Yuan, X. Z.; Tong, J. Y.; Zeng, G. M.; Li, H.; Xie, W. *Energy Fuels* **2009**, *23*, 3262–3267.
(11) Mahinpey, N.; Murugan, P.; Mani, T.; Raina, R. *Energy Fuels* **2009**, *23*, 2736–2742.
(12) Cantrell, K.; Ro, K.; Mahajan, D.; Anjom, M.; Hunt, P. G. *Ind. Eng. Chem. Res.* **2007**, *46*, 8918–8927.

pubs.acs.org/EF

which represent tremendous energy resources.[1,13] For instance, an annual 5.3 million tons of swine manure generated in the U.S. could replace about 6.0 million barrels of petroleum-based fuels after conversion processing, equivalent to 2.1% of the annual consumption of petroleum in the U.S.[14,15]

Transformation of animal manures to bioenergy can be achieved through biological and thermochemical routes.[16] Thermochemical routes clearly show the advantages of converting most organic matter into energy-rich products with processing times in the span of minutes to hours instead of days to weeks required for biological routes.[13] Pyrolysis and hydrothermal processes are two major thermochemical approaches for conversion of biomass; both lead to products including noncondensable gases (synthesis or producer gas), condensable vapors/liquids (bio-oil and tar), and solids (char and ash).[5,11,17−23] Slow pyrolysis is an established method in char production, typically using high temperatures in the range of 350−700 °C, slow heating rates of 1−20 °C/min, and long char residence times of hours to days under a non-oxygen atmosphere.[7−9,20,24] Chars generated from animal wastes can be used for heat production,[25,26] as a soil conditioner or amendment to improve soil quality,[27−29] or for immobilization of heavy metals in soil and water.[21,30,31]

Hydrothermal process covers both supercritical (hydrothermal gasification) and subcritical (hydrothermal liquefaction) temperatures. The main purpose of the supercritical hydrothermal gasification process is to produce energy gas, such as methane, whereas the main product from the subcritical hydrothermal liquefaction process is to produce oil.

Hydrothermal liquefaction and gasification, with liquid and gaseous fuels as the major products, respectively, are gaining attention.[6,10,32−39] Closely related hydrothermal carbonization (HTC) is a low-pressure−temperature area of the general liquefaction regime, as classified by Peterson et al.[36] Although the HTC process was developed as early as 1913 by Bergius,[40] it has received little attention in current biomass conversion research. It converts biomass feedstock mainly into chars and gases consisting mostly of carbon dioxide. Hydrothermal carbonization is usually performed by applying temperatures up to 250 °C in a suspension of biomass and water under weakly acidic conditions at saturated pressure for 1−72 h.[41] The HTC process removes oxygen and hydrogen from the feedstock mainly via dehydration and decarboxylation.[41] Noteworthy is that the HTC method shows distinct advantages over pyrolysis in that it can process wet biomass, thus avoiding a substantial drying cost for typically wet biomass feedstocks. Moreover, HTC provides the advantage of producing a solid fuel that is stable and nontoxic and, thus, easier to handle and store.[15,29,41,42]

Although chars made from pyrolysis and HTC have similar physical appearance, their chemical properties are different because of different carbonization processes and thermochemical reactions. For example, the char prepared from pyrolysis (hereafter called pyrochar) usually displays predominant aromatics, whereas the char produced from HTC (hereafter called hydrochar) shows mainly aliphatics.[43] Chemical characterization of char is critical to understand the different reaction mechanisms of pyrolysis and HTC processes. Furthermore, clear knowledge of char structures is important for the beneficial use of char products, which depends upon their physical and chemical characteristics.[20,44,45]

Solid-state ^{13}C nuclear magnetic resonance (NMR) spectroscopy has been frequently employed to characterize carbonaceous materials. The most commonly used ^{13}C cross-polarization magic-angle spinning (CP/MAS) technique, with the advantage of sensitivity enhancement, has significantly advanced our understanding of char chemical structures, despite its inherent drawbacks.[45−49] Recently, we have developed and applied a range of advanced solid-state ^{13}C NMR techniques to characterize various kinds of natural organic matter samples. The applications of these systematic techniques have revealed

(13) Ro, K. S.; Cantrell, K. B.; Hunt, P. G.; Ducey, T. F.; Vanotti, M. B.; Szogi, A. A. *Bioresour. Technol.* **2009**, *100*, 5466–5471.

(14) United States Department of Agriculture (USDA). *USDA Agricultural Statistics*; USDA National Agricultural Statistics Service: Washington, D.C., 2005 (www.usda.gov).

(15) Xiu, S. N.; Shahbazi, A.; Shirley, V.; Cheng, D. *J. Anal. Appl. Pyrolysis* **2010**, *88*, 73–79.

(16) Cantrell, K. B.; Ducey, T.; Ro, K. S.; Hunt, P. G. *Bioresour. Technol.* **2008**, *99*, 7941–7953.

(17) Karagoz, S.; Bhaskar, T.; Muto, A.; Sakata, Y. *Fuel* **2005**, *84*, 875–884.

(18) Liu, A.; Park, Y.; Huang, Z. L.; Wang, B. W.; Ankumah, R. O.; Biswas, P. K. *Energy Fuels* **2006**, *20*, 446–454.

(19) Mohan, D.; Pittman, C. U.; Steele, P. H. *Energy Fuels* **2006**, *20*, 848–889.

(20) Brewer, C. E.; Schmidt-Rohr, K.; Satrio, J. A.; Brown, R. C. *Environ. Prog. Sustainable Energy* **2009**, *28*, 386–396.

(21) Liu, Z. G.; Zhang, F. S.; Wu, J. Z. *Fuel* **2010**, *89*, 510–514.

(22) Laird, D. A.; Brown, R. C.; Amonette, J. E.; Lehmann, J. *Biofuels, Bioprod. Biorefin.* **2009**, *3*, 547–562.

(23) Abdullah, H.; Mediaswanti, K. A.; Wu, H. W. *Energy Fuels* **2010**, *24*, 1972–1979.

(24) Bridgwater, A. V.; Peacocke, G. V. C. *Renewable Sustainable Energy Rev.* **2000**, *4*, 1–73.

(25) Boateng, A. A. *Ind. Eng. Chem. Res.* **2007**, *46*, 8857–8862.

(26) Boateng, A. A.; Mullen, C. A.; Goldberg, N.; Hicks, K. B.; Jung, H. J. G.; Lamb, J. F. S. *Ind. Eng. Chem. Res.* **2008**, *47*, 4115–4122.

(27) Glaser, B.; Lehmann, J.; Zech, W. *Biol. Fertil. Soils* **2002**, *35*, 219–230.

(28) Laird, D. A. *Agron. J.* **2008**, *100*, 178–181.

(29) Funke, A.; Ziegler, F. *Proceedings of the 17th European Biomass Conference and Exhibition*; Hamburg, Germany, June 29−July 3, 2009; pp 1037−1050.

(30) Uchimiya, M.; Lima, I. M.; Klasson, K. T.; Wartelle, L. H. *Chemosphere* **2010**, *80*, 935–940.

(31) Uchimiya, M.; Lima, I. M.; Klasson, K. T.; Chang, S. C.; Wartelle, L. H.; Rodgers, J. E. *J. Agric. Food. Chem.* **2010**, *58*, 5538–5544.

(32) Williams, P. T.; Onwudili, J. *Energy Fuels* **2006**, *20*, 1259–1265.

(33) Zhou, D.; Zhang, L. A.; Zhang, S. C.; Fu, H. B.; Chen, J. M. *Energy Fuels* **2010**, *24*, 4054–4061.

(34) Matsumura, Y.; Minowa, T.; Potic, B.; Kersten, S. R. A.; Prins, W.; van Swaaij, W. P. M.; van de Beld, B.; Elliott, D. C.; Neuenschwander, G. G.; Kruse, A.; Antal, M. J. *Biomass Bioenergy* **2005**, *29*, 269–292.

(35) Patil, V.; Tran, K. Q.; Giselrod, H. R. *Int. J. Mol. Sci.* **2008**, *9*, 1188–1195.

(36) Peterson, A. A.; Vogel, F.; Lachance, R. P.; Froling, M.; Antal, M. J.; Tester, J. W. *Energy Environ. Sci.* **2008**, *1*, 32–65.

(37) Elliott, D. C. *Biofuels, Bioprod. Biorefin.* **2008**, *2*, 254–265.

(38) Kruse, A. *Biofuels, Bioprod. Biorefin.* **2008**, *2*, 415–437.

(39) Kruse, A. *J. Supercrit. Fluids* **2009**, *47*, 391–399.

(40) Bergius, F. *Die Anwendung hoher Drücke bei chemischen Vorgängen und eine Nachbil dung des Entstehungsprozesses der Steinkohle*; Wilhelm Knapp: Halle an der Saale, Germany, 1913; pp 41−58.

(41) Funke, A.; Ziegler, F. *Biofuels, Bioprod. Biorefin.* **2010**, *4*, 160–177.

(42) Titirici, M. M.; Thomas, A.; Antonietti, M. *New J. Chem.* **2007**, *31*, 787–789.

(43) Titirici, M. M.; Antonietti, M.; Baccile, N. *Green Chem.* **2008**, *10*, 1204–1212.

(44) Guerrero, M.; Ruiz, M. P.; Millera, A.; Alzueta, M. U.; Bilbao, R. *Energy Fuels* **2008**, *22*, 1275–1284.

(45) Baccile, N.; Laurent, G.; Babonneau, F.; Fayon, F.; Titirici, M. M.; Antonietti, M. *J. Phys. Chem. C* **2009**, *113*, 9644–9654.

(46) Sharma, R. K.; Hajaligol, M. R.; Smith, P. A. M.; Wooten, J. B.; Baliga, V. *Energy Fuels* **2000**, *14*, 1083–1093.

(47) Sharma, R. K.; Wooten, J. B.; Baliga, V. L.; Martoglio-Smith, P. A.; Hajaligol, M. R. *J. Agric. Food Chem.* **2002**, *50*, 771–783.

(48) Czimczik, C. I.; Preston, C. M.; Schmidt, M. W. I.; Werner, R. A.; Schulze, E. D. *Org. Geochem.* **2002**, *33*, 1207–1223.

(49) Bardet, M.; Hediger, S.; Gerbaud, G.; Gambarelli, S.; Jacquot, J. F.; Foray, M. F.; Gadelle, A. *Fuel* **2007**, *86*, 1966–1976.

detailed insights into the chemical structures of natural organic matter.[50−55]

The objectives of the present work were (1) to characterize swine-manure chars produced from pyrolysis and HTC under various preparation conditions using advanced solid-state ^{13}C NMR techniques and (2) to gain insights into the effects of different preparation methods and conditions on the chemical structures of swine-manure chars.

Experimental Section

Char Preparation. Raw swine-manure solid was obtained from a solid−liquid separation system treating flushed manure from a 5600-head fishing swine operation in North Carolina.[56] The dewatered swine-manure solid with typically about 25% solid was dried to 20 and 12.8% moisture contents, respectively, for the preparation of hydrochars and pyrochar, in a drying barn for a week.

One pyrochar and four hydrochars were prepared and employed in the present study. Pyrochar was produced by pyrolyzing dried swine-manure solid (12.8% solid) for 2 h at 620 °C with a heating rate of 13 °C/min using a proprietary skid-mounted batch reactor system.[59] For hydrochar, the solution of swine-manure solid (20% solid) was heated to 250 °C with a heating rate of 0.7 °C/min in a 1 L stainless-steel batch reactor system wrapped with a band heater (Parr Instrument Co., Moline, IL). The operating pressure of the system ranged from 3.4 to 9.0 MPa, representing subcritical conditions. Once the temperature of swine-manure solution reached 250 °C, it was maintained at that temperature for 20 h before the heater was turned off. Afterward, the reactor content was cooled to room temperature overnight. Hydrochar was then separated using a 1.6 μm glass microfiber filter and, subsequently, dried at 100 °C (denoted as HTC-swine W). Some of the dried hydrochar was extracted with about 1 g/4.5 mL of acetone to remove the tarry stuff deposited on hydrochar (designated as HTC-swine A and described as acetone wash). Hydrochars are intended to be used as soil amendments to improve soil fertility. However, manure hydrochars typically contain very high levels of phosphorus because of the excretion of P from animal feeds.[57] If manure chars are applied at rates typically tested by researchers (i.e., 0.4−2%), it may supersaturate soil with P. To reduce the P content of the swine-manure solid, citric acid was added to 20% solid solution of swine manure until the pH of the slurry reached ca. 3.1−3.5. Then, the mixture was stirred for 24 h. Afterward, the solid was separated using a centrifuge and dried at 100 °C. Appropriate amounts of acid-washed swine-manure solid and deionized water were mixed to make a 20% solid solution for subsequent HTC at 250 °C for 20 h. The resulting hydrochar was acetone-washed and dried (designated as HTC-AW-swine A and described as citric acid prewash and acetone wash). The P

Table 1. Proximate and Ultimate Analyses of Raw Swine-Manure Solid and Chars

parameters	raw swine-manure solid	HTC-swine A	pyrochar
Proximate Analyses[a]			
moisture (%)	12.8 ± 0.3	3.4 ± 0.8	3.4 ± 0.1
volatile matter (%$_{db}$)[b,c]	60.6 ± 1.1	59.1 ± 1.5	14.1 ± 2.5
fixed carbon (%$_{db}$)[d]	8.1 ± 0.6	13.1 ± 1.3	41.2 ± 1.3
ash (%$_{db}$)[a]	18.5 ± 0.2	27.8 ± 0.3	44.7 ± 1.2
HHV (MJ/kg)[e]	19.5 ± 0.2	NA[f]	18.3 ± 0.4
Ultimate Analyses[g]			
H (%$_{db}$)	5.9 ± 0.1	5.7 ± 0.0	1.9 ± 0.3
C (%$_{db}$)	47.3 ± 0.2	49.5 ± 2.8	50.7 ± 0.6
O (%$_{db}$)	20.1 ± 0.4	16.5 ± 6.0	< 0.01
N (%$_{db}$)	4.58 ± 0.13	1.92 ± 0.95	3.26 ± 0.08
S (%$_{db}$)	0.93 ± 0.04	NA	0.66 ± 0.01
P (mg/g of dm)[h]	23.7 ± 0.8	47.7	71.5 ± 1.3

[a] ASTM D3172. [b] ASTM D3175-07. [c] db = dry basis. [d] Calculated as 100 − volatile matter − ash. [e] HHV = higher heating value. [f] NA = not available. [g] ASTM D3176-02. [h] U.S. EPA Method 3052.

content of the hydrochars produced from the swine solid prewashed with citric acid was reduced to about 70% of that of hydrochars from non-prewashed swine solids.[58] Acids have been shown to enhance the hydrolysis reaction of feedstock, which may be the rate-determining step for HTC reactions.[29,41] We tested this process by adding citric acid until the pH of raw swine-manure solid solution became about 4.0, before it was subjected to HTC. The resulting acid-catalyzed hydrochar was then washed with acetone and dried (designated as HTC-AC-swine A and described as citric acid catalysis and acetone wash). When swine manures were handled, all proper personal protection equipments (PPEs) were worn and the glassware was washed using 10% bleach solution.

Table 1 shows proximate and ultimate analyses of the raw swine-manure solid, pyrochar,[59] and the acetone-washed swine hydrochar (HTC-swine A).

NMR Spectroscopy. ^{13}C NMR analyses were performed using a Bruker Advance III 300 spectrometer at 75 MHz (300 MHz ^{1}H frequency). All experiments were run in a double-resonance probe head using 4 mm sample rotors.

Quantitative [13]C Direct Polarization/Magic-Angle Spinning (DP/MAS) NMR. Quantitative ^{13}C DP/MAS NMR experiments were performed at a spinning speed of 13 kHz. The 90° [13]C pulse-length was 4 μs. Recycle delays, ranging from 4 to 20 s, were determined by the cross-polarization/spin−lattice relaxation time/total suppression of sidebands (CP/T_1-TOSS) technique to ensure all carbon nuclei were relaxed by more than 95%.[60] Non-protonated carbons and mobile carbon fractions were quantified using a combination of the DP/MAS technique with a recoupled dipolar-dephasing delay of 68 μs.[61] The recycle delays and numbers of scans for DP/MAS and DP/MAS with dipolar dephasing were as follows: for raw swine-manure solid, 10 s and 1024 scans; for pyrochar, 5 s and 1024 scans; for HTC-swine W, 20 s and 1024 scans; for HTC-swine A, 4 s and 1024 scans; for HTC-AW-swine A, 5 s and 1024 scans; and for HTC-AC-swine A, 10 s and 1024 scans, respectively.

[13]C Cross-Polarization/Total Suppression of Sidebands (CP/TOSS) and ^{13}C CP/TOSS Plus Dipolar Dephasing. Semiquantitative compositional information was obtained with good sensitivity using a ^{13}C cross-polarization/magic-angle spinning (CP/MAS) NMR technique (MAS, 5 kHz; CP time, 1 ms; and [1]H 90° pulse-length, 4 μs). A four-pulse total suppression of

(50) Mao, J. D.; Holtman, K. M.; Scott, J. T.; Kadla, J. F.; Schmidt-Rohr, K. *J. Agric. Food Chem.* **2006**, *54*, 9677–9686.

(51) Mao, J. D.; Cory, R. M.; McKnight, D. M.; Schmidt-Rohr, K. *Org. Geochem.* **2007**, *38*, 1277–1292.

(52) Mao, J. D.; Ajakaiye, A.; Lan, Y. Q.; Olk, D. C.; Ceballos, M.; Zhang, T. Q.; Fan, M. Z.; Forsberg, C. W. *J. Agric. Food Chem.* **2008**, *56*, 2131–2138.

(53) Mao, J. D.; Olk, D. C.; Fang, X. W.; He, Z. Q.; Schmidt-Rohr, K. *Geoderma* **2008**, *146*, 353–362.

(54) Mao, J. D.; Palazzo, A. J.; Olk, D. C.; Clapp, C. E.; Senesi, N.; Bashore, T. L.; Cao, X. Y. *Soil Sci.* **2010**, *175*, 329–338.

(55) Mao, J. D.; Schimmelmann, A.; Mastalerz, M.; Hatcher, P. G.; Li, Y. *Energy Fuels* **2010**, *24*, 2536–2544.

(56) Vanotti, M. B.; Szogi, A. A.; Millner, P. D.; Loughrin, J. H. *Bioresour. Technol.* **2009**, *100*, 5406–5416.

(57) Novak, J. M.; Lima, I.; Xing, B. S.; Gaskin, J. W.; Steiner, C.; Das, K. C.; Ahmedna, M.; Rehrah, D.; Watts, D. W.; Busscher, W. J.; Schomberg, H. *Ann. Environ. Sci.* **2009**, *3*, 195–206.

(58) *Southern Cooperative Series Bulletin 368*; Plant and Feed Analysis Lab, Agricultural Service Laboratory, Clemson University: Clemson, SC, May 1992; p 9.
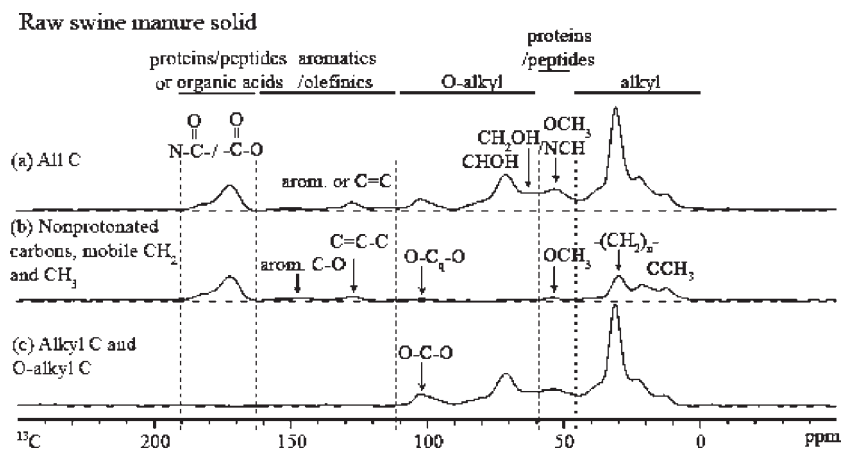
(59) Ro, K. S.; Cantrell, K. B.; Hunt, P. G. *Ind. Eng. Chem. Res.* **2010**, *49*, 10125–10131.

(60) Mao, J. D.; Hu, W. G.; Schmidt-Rohr, K.; Davies, G.; Ghabbour, E. A.; Xing, B. S. *Soil Sci. Soc. Am. J.* **2000**, *64*, 873–884.

(61) Mao, J. D.; Schmidt-Rohr, K. *Environ. Sci. Technol.* **2004**, *38*, 2680–2684.

Figure 1. ^{13}C NMR spectral editing for identification of functional groups in raw swine-manure solid. (a) Unselective CP/TOSS spectrum for reference, with a contact time of 1 ms at a spinning speed of 5 kHz. (b) Corresponding dipolar-dephased ^{13}C CP/TOSS spectrum, showing non-protonated carbons and mobile segments, acquired after 40 μs of decoupling gated off. (c) Selection of sp^3-hybridized carbon signals by a ^{13}C CSA filter, which, in particular, selects anomerics around 90–120 ppm. CSA filter time = 47 μs. The major structural moieties are listed on the top of the spectra.

sidebands (TOSS)[62] was employed before detection, with the two-pulse phase-modulated (TPPM) decoupling applied for optimum resolution. Sub-spectra for non-protonated and mobile carbon groups were obtained by combining the ^{13}C CP/TOSS sequence with a 40 μs dipolar dephasing. The numbers of scans of ^{13}C CP/TOSS and ^{13}C CP/TOSS with dipolar dephasing were 6144 for all six samples. The measuring time of ^{13}C CP/TOSS spectra was 0.9 h for raw swine-manure solid and HTC-AC-swine A and 1.4 h for pyrochar, HTC-swine W, HTC-swine A, and HTC-AW-swine A. The measuring time of the spectra of ^{13}C CP/TOSS with dipolar dephasing was 1.4 h for all six samples.

^{13}C Chemical-Shift-Anisotropy (CSA) Filter. Because O–C–O carbons (e.g., anomeric C in carbohydrate rings) and aromatic carbon resonances can overlap between 120 and 90 ppm, the aromatic carbon signals were selectively suppressed using a five-pulse ^{13}C CSA filter with a CSA-filter time of 47 μs.[63] The number of scans and measuring time were 6144 and 1.7 h, respectively, for all six samples. The recycle delay was 1.0 s.

^{1}H–^{13}C Two-Dimensional Heteronuclear Correlation (2D HETCOR) NMR. Two-dimensional HETCOR NMR experiments[64] used a Lee–Goldburg cross-polarization (LGCP) of 0.5 ms to suppress ^{1}H–^{1}H spin diffusion during polarization transfer, with a MAS of 6.5 kHz. The resulting spectra showed mostly one- and two-bond ^{1}H–^{13}C connectivities. The number of scans and measuring time were 784 and 22 h, respectively, for both HTC-swine A and HTC-swine W. The recycle delay was 1.0 s.

^{1}H–^{13}C Long-Range Recoupled H–C Dipolar Dephasing Experiments. The size of fused aromatic rings was estimated from the recoupled ^{1}H–^{13}C dipolar dephasing.[65] In short, two ^{1}H 180° pulses per rotation period prevent MAS from averaging out weak CH dipolar couplings. To detect non-protonated carbons with good relative efficiency, direct polarization/total suppression of sidebands (DP/TOSS) was used at a spinning speed of 7 kHz. The ^{13}C 90° and 180° pulse lengths were 4 and 8 μs, respectively. The recycle delays and numbers of scans were 10 s and 640 for HTC-swine A and 5 s and 1280 for pyrochar, respectively.

Results and Discussion

Major Chemical Structural Components in Raw Swine-Manure Solid and Its Chars Derived from ^{13}C CP NMR and Spectral-Editing Spectra. Three different NMR techniques,

(62) Dixon, W. T. *J. Chem. Phys.* **1982**, *77*, 1800–1809.
(63) Mao, J. D.; Schmidt-Rohr, K. *Solid State Nucl. Magn. Reson.* **2004**, *26*, 36–45.
(64) Mao, J. D.; Xing, B. S.; Schmidt-Rohr, K. *Environ. Sci. Technol.* **2001**, *35*, 1928–1934.
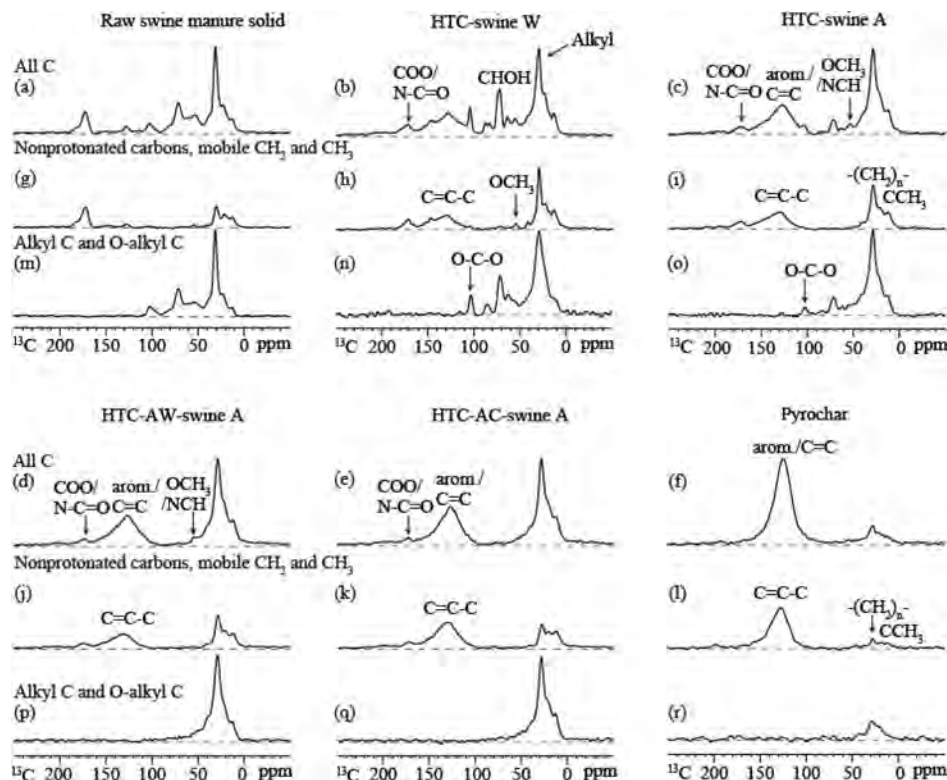(65) Mao, J. D.; Schmidt-Rohr, K. *J. Magn. Reson.* **2003**, *162*, 217–227.

^{13}C CP/TOSS, ^{13}C CP/TOSS with dipolar dephasing, and ^{13}C CSA filter, are applied to raw swine-manure solid and its chars produced from pyrolysis and HTC under various preparation conditions (Figures 1 and 2). ^{13}C CP/TOSS spectra (Figure 1a and spectra a–f of Figure 2), serving mainly as reference spectra, show the signals from potentially all carbon sites qualitatively in these samples. ^{13}C CP/TOSS with dipolar dephasing and ^{13}C CSA filter are employed to select non-protonated carbons and mobile groups, such as OCH$_3$ and CCH$_3$ groups (Figure 1b and spectra g–l of Figure 2), and sp^3-hybridized carbons (Figure 1c and spectra m–r of Figure 2), respectively.

^{13}C NMR spectra of raw swine-manure solid (Figure 1) show (i) strong and dominant signals centered around 30 ppm from resonances of alkyl carbons in the region of 0–48 ppm, (ii) NCH and OCH$_3$ signals between 48 and 60 ppm, (iii) signals as a result of CH$_2$OH groups around 62 ppm, CHOH groups around 72 ppm, and anomeric O–C–O carbons around 103 ppm in the O-alkyl region of 60–112 ppm (these peaks are typically attributed to the resonances of carbohydrates), (iv) small signals arising from aromatic carbons or olefinic C=C groups and aromatic C–O carbons in the region of 112–165 ppm, and (v) appreciable signals from COO/N–C=O groups in the 165–190 ppm region. The dipolar-dephased spectrum (Figure 1b), displaying only a very small signal from mobile OCH$_3$ groups barely above the baseline around 56 ppm, indicates that NCH carbons are the major moieties that contribute to the band between 48–60 ppm. The tiny signal of OCH$_3$ groups as well as aromatic C–O groups, which are usually attributed to lignin, indicates negligible amounts of lignin in this sample. The presence of NCH groups as well as COO/N–C=O groups demonstrates that proteins or peptides are one of the major constituents of swine manure in addition to carbohydrates. The dipolar-dephased spectrum (Figure 1b) also shows very weak signals from non-protonated anomeric O–C$_q$–O carbons and non-protonated sp^2-hybridized carbons in –C=C– double bonds (i.e., olefinics or aromatic C–C). However, significant amounts of mobile carbon groups, such as CCH$_3$ and –(CH$_2$)$_n$–, are observed in the alkyl region around 0–48 ppm. The ^{13}C CSA filter spectrum (Figure 1c) displays the signals from sp^3-hybridized carbons only, which can be used to distinguish resonances of anomeric carbons (O–C–O) from those of aromatic carbons in the region between 90 and 120 ppm. A comparison of

Figure 2. ^{13}C NMR spectral editing for identification of functional groups in raw swine-manure solid (a, g, and m), HTC-swine W (b, h, and n), HTC-swine A (c, i, and o), HTC-AW-swine A (d, j, and p), HTC-AC-swine A (e, k, and q), and pyrochar (f, l, and r). (a–f) Unselective CP/TOSS spectra. (g–l) Corresponding dipolar-dephased CP/TOSS spectra. (m–r) Selection of sp^3-hybridized carbon signals by a ^{13}C CSA filter.

the intensity of the O−C−O signal in the ^{13}C CSA filter spectrum (Figure 1c) to those in the reference CP/TOSS and dipolar-dephased spectra (spectra a and b of Figure 1) indicates that the peak centered at 103 ppm is mostly due to protonated anomeric O−CH−O carbons. The spectral features of raw swine-manure solid are very similar to those of the nontransgenic Yorkshire pig manures reported by Mao et al. (see Figure 2[52]). ^{13}C NMR spectra of both studies show that carbohydrates and proteins or peptides are the major components in swine-manure samples. Mao et al.[52] demonstrated the presence of lipids (mainly free fatty acids) in swine manures via a spectral comparison to a model compound 1-palmitoyl-2-oleoyl-*sn*-glycero-3-phosphocholine (POPC). Lipids, such as fatty acids or fats, are also major components of raw swine-manure solid in the present study, as indicated by the presence of their characteristic peaks at 13 ppm (methyl end chain *ω*), 22 ppm (methylene carbons next to the methyl end carbons, *ω*-1), 31 ppm (mobile methylene carbons, *ω*-2), 130 ppm (olefinic carbons), and 172 ppm partly arising from ester groups (Figure 1b; see Figure 3[52]).

The spectra (spectra b, h, and n of Figure 2) of the HTC-swine W (control hydrochar) without any acid prewash, catalysis, and acetone wash steps share some similarities with those of raw swine-manure solid in the sp^3-hybridized carbon region (0−112 ppm). Noticeable differences are the appreciable increase in the aromatics or −C=C− carbons around 130 ppm and the decrease in the COO/N−C=O functionalities (165−190 ppm). The comparison of the dipolar-dephased spectrum of HTC-swine W char (Figure 2h) to that of raw swine-manure solid (Figure 2g) clearly shows the increase in non-protonated sp^2-hybridized carbons, including aromatic C−C or non-protonated −C=C− as well as aromatic C−O carbons in the region of 112−165 ppm.

An interesting finding is the substantial increase in amounts of mobile −(CH$_2$)$_n$− groups in HTC-swine W char, as indicated by the dominant band around 30 ppm in its dipolar-dephased spectrum (Figure 2h). The ^{13}C CSA-filtered sub-spectrum (Figure 2n) also shows the signals almost exclusively from protonated anomeric O−CH−O carbons between 92 and 112 ppm, because barely observable signals are found within this region in the dipolar-dephased spectrum (Figure 2h). The decrease of carbohydrate signals between 60 and 112 ppm is also noticeable.

The CP/TOSS spectrum of HTC-swine A with acetone wash (Figure 2c) shows a further increase of aromatic carbons or olefinic −C=C− and aromatic C−O carbons but a substantial loss of signals assigned to O-alkyl components. Its dipolar-dephased spectrum (Figure 2i) generally shows two major bands, one from sp^3-hybridized mobile −(CH$_2$)$_n$− and CCH$_3$ groups between 0 and 48 ppm and another from sp^2-hybridized non-protonated aromatics or olefinics and aromatic C−O groups centered around 130 ppm; a small band as a result of COO/N−C=O groups is present around 172 ppm. Note that mobile −(CH$_2$)$_n$− around 30 ppm of HTC-swine A (Figure 2i) is pronouncedly reduced in comparison to that of the dipolar-dephased spectrum of HTC-swine W (Figure 2h), indicating that some mobile −(CH$_2$)$_n$− groups are removed by acetone wash. The ^{13}C CSA-filtered sub-spectrum (Figure 2o) shows a small but visible signal from protonated anomeric O−CH−O carbons between 92 and 112 ppm (Figure 2i).

The ^{13}C CP/TOSS spectrum of HTC-AW-swine A with citric acid prewash and acetone wash (Figure 2d) and that of HTC-AC-swine A with citric acid catalysis and acetone wash (Figure 2e) are very similar to each other. These spectra are composed of two broad bands representing sp^3-hybridized
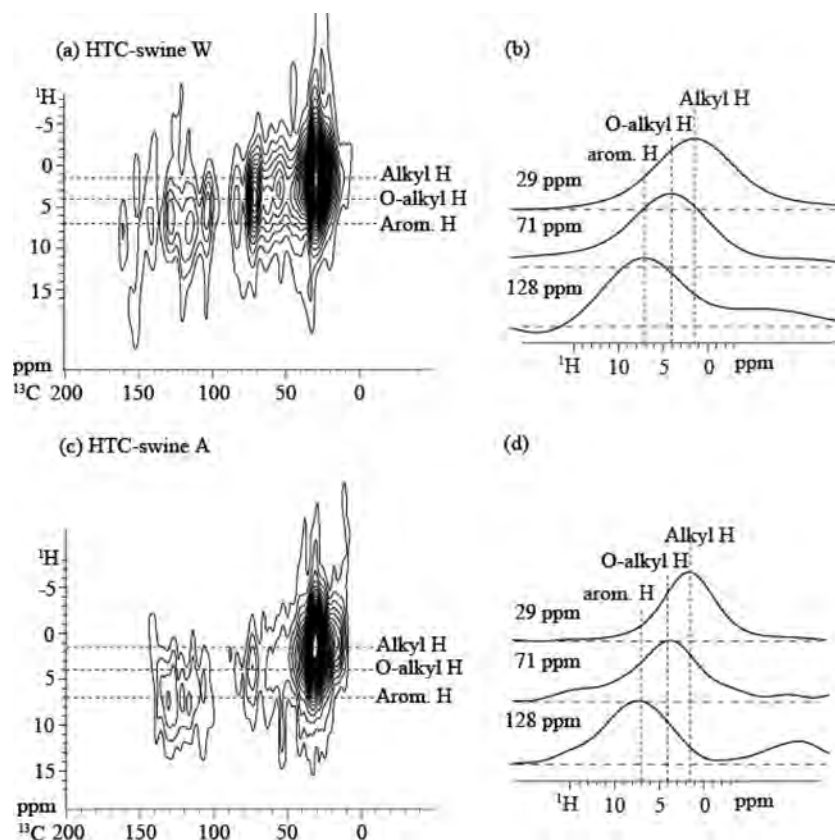
Figure 3. 2D ^{1}H$-^{13}$C HETCOR spectra of (a) HTC-swine W and (c) HTC-swine A. Right-column spectra are ^{1}H slices extracted at 29, 71, and 128 ppm for the (b) 2D HETCOR spectrum of panel a and (d) 2D HETCOR spectrum of panel c.

carbons (0−92 ppm) and sp^2-hybridized carbons (92−220 ppm), quite resembling the spectra of geological samples, such as kerogen and coal (especially HTC-AC-swine A).[55,66] Their CP/TOSS spectra (spectra d and e of Figure 2) are also similar to that of HTC-swine A, except that the peaks representing O-alkyl compounds, such as carbohydrates (60−112 ppm), in the CP/TOSS spectra of HTC-AW-swine A and HTC-AC-swine A are totally absent. The dipolar-dephased spectra (spectra j and k of Figure 2) are extremely similar to each other and resemble that of HTC-swine A, except that HTC-swine A contains more mobile −(CH$_2$)$_n$− around 30 ppm. Anomeric O−C−O carbons around 103 ppm are undetectable in their corresponding CSA-filtered spectra (spectra p and q of Figure 2), indicating that the signals in the region of 92−112 ppm are wholly attributed to aromatic carbons and all carbohydrates are removed from HTC-AW-swine A and HTC-AC-swine A. There are only slight differences between HTC-AW-swine A and HTC-AC-swine A. We observe a small shoulder around 53 ppm in the CP/TOSS spectrum of HTC-AW-swine A (Figure 2d) but not in that of HTC-AC-swine A. This small band is attributed to NCH because it is totally dephased in the dipolar-dephased spectrum (Figure 2i). HTC-AW-swine A still contains residual peptides/proteins but not HTC-AC-swine A.

In contrast, the spectra of pyrochar (spectra f, l, and r of Figure 2) are distinctly different from those of raw swine-manure solid and hydrochars. Pyrochar prepared at 620 °C for 2 h is predominantly aromatic, with only very small peaks

assigned to alkyls (0−48 ppm). The dipolar-dephased spectrum (Figure 2l) displays a very pronounced signal from non-protonated aromatic carbons but only weak signals assigned to mobile −(CH$_2$)$_n$− and CCH$_3$ components. The signals assigned to anomeric O−C−O carbons around 103 ppm completely disappear in the CSA-filtered spectrum (Figure 2r), indicating the absence of carbohydrates in pyrochar. In addition, this char does not contain any peptides or proteins either, as demonstrated by the lack of NCH around 53 ppm and N−C=O around 172 ppm.

Connectivities of Different Functional Groups in Hydro-chars from Short-Range ^{1}H$-^{13}$C 2D HETCOR NMR. Hydrochars, HTC-swine W, and HTC-swine A contain more abundant functional groups than pyrochar and other hydrochars. Therefore, these two chars are selected for ^{1}H$-^{13}$C 2D HETCOR experiments to investigate the connectivities of different functional groups, especially to examine whether different components are closely associated with each other. Panels a and c of Figure 3 display the ^{1}H$-^{13}$C 2D HETCOR spectra of HTC-swine W and HTC-swine A with 0.5 ms of LGCP, respectively, which show correlation peaks for protons and ^{13}C nuclei that are connected by a ^{13}C$-^1$H coupling over primarily one and two bonds. Proton cross-sections (panels b and d of Figure 3) at specific ^{13}C chemical shifts of 29, 71, and 128 ppm were extracted from the spectra to aid in the identification of connectivities or proximities of different functional groups. For both HTC-swine W and HTC-swine A, the ^{13}C signal around 29 ppm attributed to primarily −(CH$_2$)$_n$− carbons has an interaction with the ^{1}H signal around 1.5 ppm derived from protons directly attached to alkyl carbons, i.e., with their own protons. At the ^{13}C chemical shift of approximately 71 ppm, where OCH

(66) Mao, J. D.; Fang, X. W.; Lan, Y. Q.; Schimmelmann, A.; Mastalerz, M.; Xu, L.; Schmidt-Rohr, K. *Geochim. Cosmochim. Acta* **2010**, *74*, 2110−2127.

carbons are located, a strong contribution from protons resonating at approximately 4 ppm is observed, indicating that OCH carbons are associated mostly with their directly attached protons for both chars. The ^1H slices at 7 ppm extracted at the ^{13}C chemical shift of ~128 ppm also show signals mainly from aromatic protons. Alkyl, OCH (mostly from carbohydrates), and aromatic carbons are primarily correlated with their directly attached protons, indicating that they are mainly separated from each other and suggesting that alkyls, carbohydrates, and aromatics are primarily isolated components in these two samples.

Aromatic Cluster Sizes from $^1H-^{13}C$ Recoupled Long-Range Dipolar Dephasing. Aromatic components are shown to increase significantly, although to a different extent, in the structures of hydrochars and pyrochar compared to that of raw swine-manure solid. Strongly distance-dependent $^1H-^{13}C$ long-range dipolar dephasing[65] provides information about distances of the aromatic carbons from protons at the edge of the condensed aromatic ring system. The larger the average $^1H-^{13}C$ distance, the slower the dephasing of the ^{13}C signal and, thus, the larger the aromatic cluster size. $^1H-^{13}C$ long-range recoupled dipolar dephasing experiments are applied to only HTC-swine A and pyrochar. We choose these two samples because the aromatic feature of HTC-swine A is very similar to that of other hydrochars (except HTC-AC-swine A), whereas that of pyrochar is distinct. We skip this experiment for raw swine-manure solid because of its very insignificant aromatics. We also include previously characterized lignin for comparison.[65] Panels a and b of Figure 4 show a series of DP/TOSS spectra of HTC-swine A and pyrochar, respectively, with different dephasing times. The dephasing times of HTC-swine A range from 0.29 to 0.86 ms, whereas those of pyrochar are from 0.29 to 1.43 ms. At the dephasing time of 0.86 ms, no signal for aromatic carbons is left for HTC-swine A, while the aromatic peak is still quite obvious for pyrochar, accounting for ~20% of its original intensity. Note that the residual bands in the alkyl region of HTC-swine A are due to the high mobility of the CCH_2C and CCH_3 groups. The dephasing curves of HTC-swine A, pyrochar, and lignin are shown in Figure 4c. The dephasing rates, which reflect both the distance from and number of the nearest protons, are in order of lignin > HTC-swine A > pyrochar. This is indicative of the presence of fused or more substituted aromatic rings in both hydrochars and pyrochar than lignin but a more condensed character of aromatics in pyrochar than HTC-swine A.

Quantitative Compositions Based on DP/MAS and DP/MAS with Recoupled Dipolar Dephasing Spectra. Figure 5 shows the quantitative DP/MAS spectra (top) and corresponding DP/MAS with recoupled dipolar dephasing spectra (bottom) of raw swine-manure solid and chars produced under different carbonization conditions. The DP/MAS technique provides quantitative structural information on the whole structure, and the dipolar-dephased spectra are used to estimate the relative amounts of protonated and non-protonated aromatic or $-C=C-$ carbons and mobile $-OCH_3$ groups. On the basis of the ^{13}C NMR peak assignments from previously described spectral editing techniques and the study on swine-manure samples by Mao et al.,[52] we derive quantitative compositions of the carbons of all six samples (Table 2).

The dominant component in raw swine-manure solid is alkyl (62.7%), followed by O-alkyl (excluding OCH_3, such as those of carbohydrates) (12.6%), COO/N−C=O (11.0%),
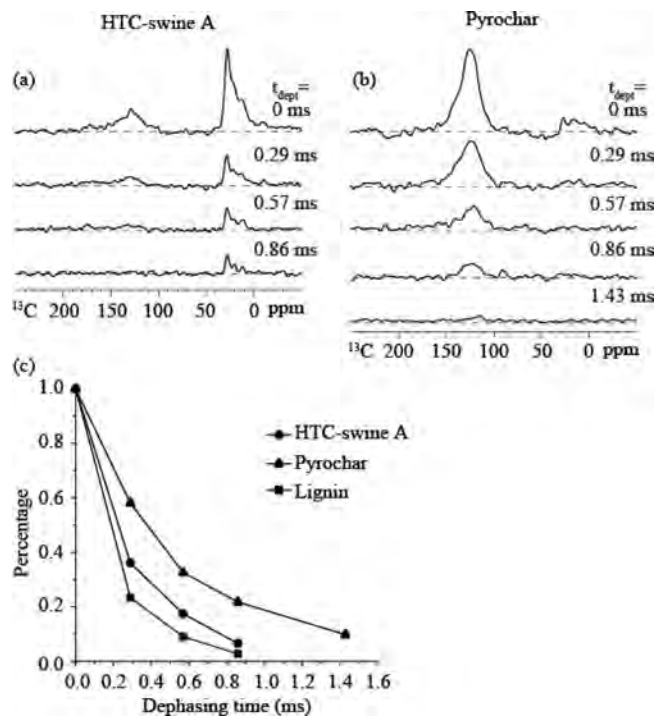

Figure 4. Series of DP/TOSS spectra after $^1H-^{13}C$ recoupled long-range dipolar dephasing of the indicated durations t_{deph} of (a) HTC-swine A and (b) pyrochar. (c). Long-range dipolar dephasing curves for HTC-swine A and pyrochar. The aromatic signals were integrated between 107 and 142 ppm: (●) HTC-swine A, (▲) pyrochar, and (■) lignin. For reference, data for lignin[65] are also shown. The data points have been corrected for regular T_2 relaxation.

and NCH (5.9%) groups, representative of constituents of primarily biomass materials, such as lipids, carbohydrates, and proteins/peptides. In comparison to raw swine-manure solid, alkyl carbons generally display a decreasing trend but still represent the most abundant carbon species (46.2−62.6%) in hydrochars from HTC-swine A, HTC-swine W, and HTC-AW-swine A to HTC-AC-swine A. The decline of O-alkyl (excluding OCH_3), COO/N−C=O, NCH, and OCH_3 groups is also observed. In contrast, aromatic/olefinic groups (both protonated and non-protonated) and aromatic C−O groups increase substantially.

Hydrochars generated under different processing conditions also vary in the distributions of different functional groups. Although the percentage of alkyl carbons of the HTC-swine W is similar to that of raw swine manure, the percentages of aromatic/olefinic (both protonated and non-protonated) and aromatic C−O carbons are significantly increased. In addition, the percentages of carbohydrate (O-alkyl), COO/N−C=O, and NCH carbons are substantially reduced. This increase in aromatic carbons accompanying the decrease in carbohydrates and proteins/peptides indicates that the carbonization process has taken place to a certain extent. The distribution of chemical functional groups of HTC-swine A is different from that of HTC-swine W, with a substantial decrease in O-alkyls and some decline in NCH and COO/N−C=O as well as a corresponding increase in aromatics/olefinics, suggesting that acetone substantially removes carbohydrates and peptides of the hydrochar. Moreover, OCH_3 groups are totally removed in HTC-swine A with just acetone wash. With citric acid prewash and acetone wash (HTC-AW-swine A), aromatic C−O and aromatics/olefinics are increased and alkyls are decreased,
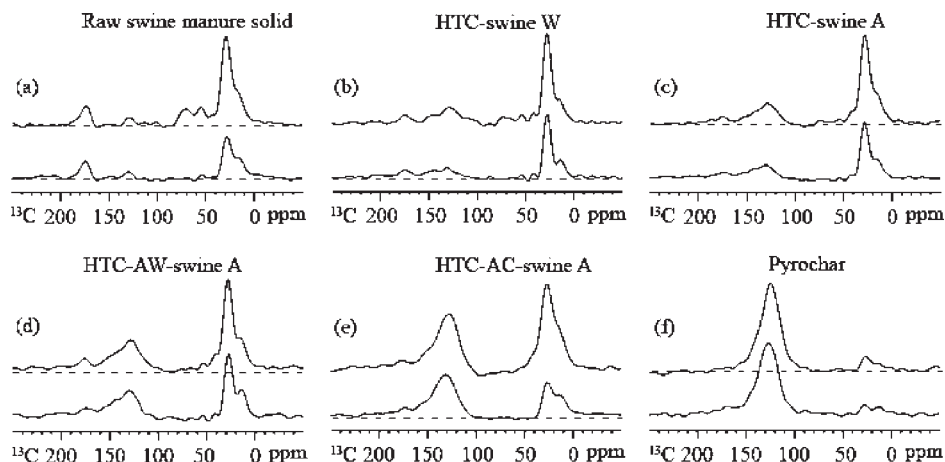
Figure 5. Quantitative DP/MAS ^{13}C NMR of all C and DP/MAS after recoupled dipolar dephasing showing non-protonated C plus mobile groups: (a) raw swine-manure solid, (b) HTC-swine W, (c) HTC-swine A, (d) HTC-AW-swine A, (e) HTC-AC-swine A, and and (f) pyrochar.

Table 2. Quantitative Structural Information of Raw Swine-Manure Solid and Chars^a

sample	190−220 ppm aldehyde/ ketone	165−190 ppm COO/ N−C=O	165−145 ppm aromatic C−O	112−145 ppm^b non-protonated aromatic/ olefinic C	protonated aromatic/ olefinic C	112−60 ppm O-alkyl C	60−48 ppm NCH	O−CH$_3$	48−0 ppm alkyl
raw swine-manure solid	1.1	11.0	0.5	3.2	1.7	12.6	5.9	1.2	62.7
HTC-swine W	2.1	6.0	4.4	11.5	6.1	6.6	2.6	0.7	59.9
HTC-swine A	1.8	5.6	5.2	14.1	7.0	1.8	1.8	0	62.6
HTC-AW-swine A	1.7	5.7	6.9	18.3	9.2	0.0	1.6	0	56.6
HTC-AC-swine A	3.7	5.3	8.1	28.1	7.7	0.0	0.9	0	46.2
pyrochar	0.9	2.8	6.4	54.9	20.7	2.2	1.1	0	11.0

^{a} Sidebands are corrected and added to the centerband based on methods provided by Mao and Schmidt-Rohr,[61] and Mao et al.[60] The percentages in each row add up to 100. ^{b} Note that, for raw swine-manure solid, HTC-swine W, and HTC-swine A, the spectral range of 112−145 ppm is assigned to aromatic carbons. For HTC-AW-swine A, HTC-AC-swine A, and pyrochar, the signals from anomeric O−C−O carbons are absent from the subspectra (spectra p−r of Figure 2) obtained by ^{13}C CSA filter and, thus, aromatic carbons are acquired by integrating the spectral range of 92−145 ppm.

with O-alkyls totally removed in comparison to just acetone wash (HTC-swine A). After citric acid catalysis and acetone wash (HTC-AC-swine A), aromatic C−O and non-protonated aromatics/olefinics are further increased and alkyls are further decreased, with protonated aromatics and NCH slightly decreased in comparison to citric acid prewash and acetone wash (HTC-AW-swine A). Note that O-alkyl carbons (1.8% in HTC-swine A) are totally lost in HTC-AW-swine A and HTC-AC-swine A chars probably because of enhanced hydrolysis of carbohydrates in raw swine manure by citric acid catalysis. The contents of COO/N−C=O groups do not seem to change much with different hydrothermal processes and remain to be relatively small (5.3−6.0%) in these chars.

It should be noted that the ratios of non-protonated to protonated aromatic/olefinic carbons for HTC-swine W, HTC-swine A, and HTC-AW-swine A are quite similar and ca. 2. However, this ratio for HTC-AC-swine A is 3.6. Obviously, citric acid catalysis and acetone wash (HTC-AC-swine A) provide deeper carbonization than other HTC processing.

For the char prepared from pyrolysis at 620 °C for 2 h, it displays wholly different structural features. Aromatic carbons (82.0%) become the predominant components, with the remainder being mainly alkyl carbons (11.0%). Furthermore, about 75% of total aromatic carbons (including aromatics and aromatic C−O groups) are not protonated. The amount of oxygen-bearing groups, except that of aromatic C−O carbons, decreases dramatically compared to raw swine manure, because of the loss of O-alkyls and COO/N−C=O groups. The contents of NCH groups, typical of

peptides and proteins, are substantially declined because of high-temperature pyrolysis, supporting the 68% N loss observed during the swine-manure pyrolysis reaction.[59] In agreement with the results from the ^{1}H−^{13}C recoupled long-range dipolar dephasing curve, these quantitative data indicate that swine manure heated at 620 °C forms a char that is more aromatic and carbonaceous in nature than chars produced under hydrothermal conditions.

Related Processes during HTC. The reaction mechanisms involved in HTC are still not well-understood because of their complexity. Aided by the reaction mechanisms summarized in two reviews,[36,41] we attempt to relate the detailed structural information obtained by advanced solid-state ^{13}C NMR to possible reaction mechanisms.

Hydrolysis of Proteins. Peptide bonds that usually occur between amino acids rapidly hydrolyze in hydrothermal systems, and the optimal yields of amino acids were reported at ca. 250 °C.[36] Amino acids produced from hydrolysis can readily dissolve in water and, thus, be removed from the solid products. This process explains the parallel reduction of COO/N−C=O and NCH groups in the HTC-swine W. Furthermore, because citric acid can enhance the hydrolysis reactions, these N-containing groups are further reduced in HTC-AW-swine A and HTC-AC-swine A.

Hydrolysis of Fats. Triacylglycerides (TAGs) are the most common form of fats and oils in biological systems and can be hydrothermally split into three fatty acids and glycerol.[36] Free fatty acids could undergo further decomposition (decarboxylation, etc.), but the extent of such a process is

unknown at this time. Holliday et al.[67] studied the hydrolysis of vegetable oils at the temperatures of 250−375 °C and concluded that free fatty acids were stable in subcritical water at temperatures below 300 °C. Short-chain fatty acids are soluble in water, which may partially explain the significant reduction in COO/N−C=O groups in HTC-swine W compared to raw swine-manure solid. Note that mobile −$(CH_2)_n$− groups in HTC-swine W are significantly more enriched than those in raw swine manure, as demonstrated by their dipolar-dephased spectra (panels g and h of Figure 2). These signals are reduced in HTC-swine A (Figure 2i) and further decreased in HTC-AW-swine A (Figure 2j) and HTC-AC-swine A (Figure 2k). We are not clear about their structures at this stage. We speculate that they could be long-chain fatty acids and/or wax-like materials, which are insoluble in water but partially soluble in acetone. Some of them may be bonded to aromatics; the catalysis of citric acid changes the structures of aromatics and may render these aromatic-bonded −$(CH_2)_n$− groups more soluble.

Degradation of Carbohydrates. Carbohydrates break down under hydrothermal conditions to form monomers, such as glucose, fructose, and xylose. Subsequent reactions of these monomers lead to different major products depending upon the starting material. For example, fructose initially forms a dehydrated intermediate, 5-hydroxymethyl-2-furaldehyde (HMF), while pentose, such as xylose, dehydrates into furfural.[36,43,68] Possible dehydration products include HMF, 1,6-anhydroglucose,[69] glycolaldehyde, pyruvaldehyde, etc.[36,70,71] Degradation of carbohydrates is indicated by the disappearance of characteristic peaks of carbohydrates (∼62 ppm, CH_2OH groups; ∼72 ppm, CHOH groups; and ∼103 ppm, anomeric O−C−O carbons) in ^{13}C NMR spectra (Figures 2 and 5). While these intermediates readily dissolve in water and cause the loss of carbons, they may also condense to form insoluble particles.[29]

Aromatization. An increased aromatic portion is remarkable in hydrochars compared to raw swine-manure solid. The increase of the aromaticity during HTC is usually related to the lignin portion in biomass. However, ^{13}C CP and DP NMR spectra demonstrate that very little amount of lignin compounds, if there are any, are present in raw swine-manure solid because there are very few OCH_3 and aromatic C−O groups in the dipolar-dephased spectra. This observation undoubtedly excludes the possibility of increased aromatic compounds because of the accumulation of lignin in the present study. Baccile et al.,[45] who characterized amorphous carbonaceous materials from HTC processing of glucose at temperatures < 350 °C, pointed out that NMR resonances in the region of 110−150 ppm may not be assigned to fused six-membered aromatic rings as commonly accepted. Instead, they[45] identified furan rings cross-linked by the domains containing short keto-aliphatic chains as the structural units in the sp²-hybridized C region. In the present study, the ^{13}C NMR spectra (Figures 2 and 5) of the products from HTC processing do not show prominent peaks around 110 and 150 ppm that are assigned to C-3/C-4 and C-2/C-5,

respectively, of furan rings, excluding the assignments of these aromatics to furan. Our long-range dipolar dephasing results also indicate that the aromatics in HTC-swine A are fused six-membered aromatic rings. In addition, the formation of phenolic compounds was identified from hydrothermal degradation of the cellulose around 250−400 °C,[72] xylose under acidic conditions at 300 °C,[73] and HMF and D-fructose at 290−400 °C,[74] further confirming the possibility of six-membered aromatic rings as the main structural units in hydrochars. Condensation polymerization, specifically aldol condensation,[69,72,73] may play a major role in the formation of aromatic compounds during the HTC process.

Effects of Preparation Conditions on Char Structures. Acetone washing is an attempt to remove tarry substances along with HTC byproduct chemicals that may have been adsorbed on the hydrochar surfaces. The differences observed between the hydrochars with and without acetone washing (HTC-swine W and HTC-swine A) include the decrease of O-alkyl, NCH, and COO/N−C=O carbons, as well as relative increment of aromatic and aromatic C−O carbons. We attribute these observations to the properties of acetone as a good solvent to remove the soluble intermediates, such as monosaccharides and peptides, deposited on the hydrochar.

Hydrothermal carbonization reactions are sensitive to pH. Generally, a pH value of below 7 is required for the hydrothermal carbonization. Alkaline conditions lead to products with significantly higher H/C ratios and are commonly used in biomass liquefaction.[29] In addition, acidic conditions catalyze dehydration and improve the overall reaction rate of hydrothermal carbonization.[36,41,42] In the present study, hydrochars that have undergone citric acid prewash and catalysis (HTC-AW-swine A and HTC-AC-swine A) both show increased aromatic compounds but less alkyl compounds and the complete loss of carbohydrates compared to HTC-swine W and HTC-swine A. This effect is more pronounced in the citric acid catalysis treatment than acid prewash treatment, as indicated by the substantially higher amount of aromatic carbons but lower alkyl carbons in HTC-AC-swine A, especially a higher ratio of non-protonated to protonated aromatics/olefinics. We speculate that the residual citric acid not completely removed from the citric-acid-washed swine-manure solid may have played a catalyst role during HTC to some extent.

Pyrolysis of swine-manure solid produces pyrochar with very distinct chemical structures than those of hydrochars. Studies that investigated the structural evolution of different biomass and biomass-derived materials during pyrolysis showed that the general spectral features of the ^{13}C CP NMR spectra of chars from heating with temperatures about 600 °C were very similar.[47,75−78] Generally, these ^{13}C CP NMR spectra of chars are composed of resonances associated with predominantly aromatic carbons but very few or no alkyl carbons after exposure to high temperatures.

(67) Holliday, R. L.; King, J. W.; List, G. R. *Ind. Eng. Chem. Res.* **1997**, *36*, 932–935.

(68) Yao, C.; Shin, Y.; Wang, L. Q.; Windisch, C. F.; Samuels, W. D.; Arey, B. W.; Wang, C.; Risen, W. M.; Exarhos, G. J. *J. Phys. Chem. C* **2007**, *111*, 15141–15145.

(69) Kabyemela, B. M.; Adschiri, T.; Malaluan, R. M.; Arai, K. *Ind. Eng. Chem. Res.* **1999**, *38*, 2888–2895.

(70) Bonn, G.; Bobleter, O. *J. Radioanal. Chem.* **1983**, *79*, 171–177.

(71) Srokol, Z.; Bouche, A. G.; van Estrik, A.; Strik, R. C. J.; Maschmeyer, T.; Peters, J. A. *Carbohydr. Res.* **2004**, *339*, 1717–1726.

(72) Nelson, D. A.; Molton, P. M.; Russell, J. A.; Hallen, R. T. *Ind. Eng. Chem. Prod. Res. Dev.* **1984**, *23*, 471–475.

(73) Nelson, D. A.; Hallen, R. T.; Theander, O. *ACS Symp. Ser.* **1988**, *376*, 113–118.

(74) Luijkx, G. C. A.; Vanrantwijk, F.; Vanbekkum, H. *Carbohydr. Res.* **1993**, *242*, 131–139.

(75) Freitas, J. C. C.; Bonagamba, T. J.; Emmerich, F. G. *Carbon* **2001**, *39*, 535–545.

(76) Zhang, X. Q.; Golding, J.; Burgar, I. *Polymer* **2002**, *43*, 5791–5796.

(77) Sharma, R. K.; Wooten, J. B.; Baliga, V. L.; Hajaligol, M. R. *Fuel* **2001**, *80*, 1825–1836.

(78) Sharma, R. K.; Wooten, J. B.; Baliga, V. L.; Lin, X. H.; Chan, W. G.; Hajaligol, M. R. *Fuel* **2004**, *83*, 1469–1482.

Pyrochar in the present study also exhibits similar structural features.

Chemical structures of pyrochar differ dramatically from those of raw swine-manure solid, indicating thermal decomposition and depolymerization of its main structural constituents (fats, carbohydrates, and proteins) and subsequent formation of aromatic rings. Raw swine-manure solid undergoes substantially deeper carbonization during the pyrolysis than the HTC processes, as indicated by its higher aromatics (especially non-protonated aromatics), low alkyl, and fewer oxygen-containing groups. Note that decarboxylation occurs readily under pyrolysis conditions, leading to the loss of carboxylic signals.

Conclusions

The detailed, advanced solid-state ^{13}C NMR analyses of raw swine-manure solid and its hydrochars and pyrochar provide deep insights into their chemical structures and potential mechanisms behind their productions. (1) Pyrochar from slow pyrolysis is chemically distinct from hydrochars. Aromatics are the most dominant component in the pyrochar, with the small remainder being primarily alkyl carbons, whereas hydrochars contain mainly alkyl moieties. The increase in aromaticity during HTC treatments is much less prominent than that in pyrolysis. In addition, the aromatic cluster size of pyrochar is larger than those of hydrochars. (2) Hydrochars generated under different processing conditions vary in their chemical structures. Washing hydrochar with acetone (HTC-swine A) removes the soluble intermediates deposited on hydrochar, such as peptides and residual monomers of hemicellulose and cellulose and their degradation products. This is demonstrated by the decrease of carbohydrates and NCH and N−C=O carbons and corresponding increase of aromatic/olefinic carbons. In addition, acetone wash completely removes OCH$_3$ groups. (3) In comparison to just acetone wash (HTC-swine A), citric acid prewash and acetone wash (HTC-AW-swine A) increase aromatic C−O and aromatics/olefinics and decrease alkyls, with O-alkyls totally removed. (4) With citric acid catalysis and acetone wash (HTC-AC-swine A), aromatic C−O and non-protonated aromatics/olefinics are further increased and alkyls are further decreased, with protonated aromatics and NCH slightly decreased in comparison to citric acid prewash and acetone wash (HTC-AW-swine A). (5) The ratios

of non-protonated to protonated aromatic/olefinic carbons for HTC-swine W, HTC-swine A, and HTC-AW-swine A are all ca. 2. However, this ratio for HTC-AC-swine A is 3.6. Obviously, citric acid catalysis and acetone wash (HTC-AC-swine A) provide deeper carbonization than other HTC processing, probably because of citric acid catalysis. (6) Hydrothermal carbonization processes are associated with the hydrolysis and subsequent decomposition of major biopolymer components, such as fats, proteins, and carbohydrates, in swine manure. Condensation polymerization of the intermediates from the degradation of carbohydrates may play a major role in the formation of six-membered aromatic rings during HTC processes.

Nomenclature

NMR = nuclear magnetic resonance

TOSS = total suppression of sidebands

CP/TOSS = cross-polarization/total suppression of sidebands

CP = cross-polarization

CP/T$_1$-TOSS = cross-polarization/spin−lattice relaxation time/total suppression of sidebands

CP/MAS = cross-polarization/magic-angle spinning

PPE = personal protection equipment

DP/MAS = direct polarization/magic-angle spinning

TPPM = two-pulse phase-modulated

CSA = chemical-shift anisotropy

2D HETCOR = two-dimensional ^{1}H−^{13}C heteronuclear correlation nuclear magnetic resonance

LGCP = Lee−Goldburg cross-polarization

HTC = hydrothermal carbonization

DP/TOSS = direct polarization/total suppression of sidebands

POPC = 1-palmitoyl-2-oleoyl-*sn*-glycero-3-phosphocholine

HMF = 5-hydroxymethyl-2-furaldehyde